(This is a sample cover image for this issue. The actual cover is not yet available at this time.)

International Journal of Heat and Mass Transfer 55 (2012) 2807–2812

Contents lists available at SciVerse ScienceDirect

International Journal of Heat and Mass Transfer

journal homepage: www.elsevier.com/locate/ijhmt

Fluidic laser beam shaper by using thermal lens effect

Hong Duc Doan *, Yoshihiko Akamine, Kazuyoshi Fushinobu

Department of Mechanical and Control Engineering, Tokyo Institute of Technology, Box I6-3, Meguro-ku, Tokyo 152-8550, Japan

ARTICLE INFO

Article history:
Received 15 January 2011
Received in revised form 8 February 2012

Keywords:
Fluidic laser beam shaper
Thermal lens effect
Pump power
Propagation distance

ABSTRACT

Laser measurement and laser processing techniques have been gaining strong attention from various applications. This research aims at the development of a fluidic laser beam shaper, and in order to fulfill the objective, thermal lens effect characteristics are studied. This phenomenon has the optical property of a divergent lens since the refractive index distribution on the optical axis is formed when a liquid is irradiated. In this research, effects of the pump power and the propagation distance to the probe beam profile are investigated experimentally and theoretically, with the purpose of developing a fluidic laser beam shaper. It is indicated that, by controlling some parameters in thermal lens system such as the pump power (in the regime of linear optics) and absorption coefficient, an input Gaussian beam can be converted into a flat-top beam profile. The relationship between the distance to obtain the flat-top beam, the pump power and absorption coefficient is investigated to show the flexibility of the fluidic laser beam shaper in many fields of laser application.

1. Introduction

Gordon et al. [1] reported that the beam shape of an incident laser light expands after passing through a liquid medium. This phenomenon was termed as "the thermal lens effect". More recently, the thermal lens effect has become a well-known photo-thermal phenomenon. Phenomenological, optical, and spectroscopic studies of the thermal lens effect have been carried out to describe nonlinear defocusing effect [2–8]. Recent progress in laser technology lead to the improvement on research on thermal lens effect. Based on these efforts, other mechanisms, such as liquid density, electronic population, and molecular orientation, have been found to play an important role as well as thermal lens effect. Recent studies considering these phenomena are generally called "the transient lens effect" [9,10]. The main advantage of using the transient lens effect in Photo-Thermal-Spectroscopy is that the sensitivity is 100 to 1000 time greater than a traditional absorptiometry [11].

In this research, a new idea of applying the thermal lens effect in order to develop fluidic optical device is proposed. A schematic of the concept is shown in Fig. 1. A rectangular solid region shown in Fig. 1a represents the liquid medium, which has a temperature field generated by a heater-heat sink system or laser-induced absorption. By controlling the temperature field as well as the refractive index distribution of the liquid medium, the refractive angle of each light ray passing through the liquid medium can be controlled in order to develop fluidic optical devices such as: optical switching in Fig. 1a, beam shaper in Fig. 1b and lens in Fig. 1c. Merits of these devices include flexibility of optical parameters, versatility and low cost. In this research, it is assumed that the change of refractive index is caused only by the temperature change of the liquid medium. The authors have examined the effect of one dimensional temperature profile perpendicular to the incident beam direction and the resulting natural convection on the beam bending [12]. A 2D model in cylindrical coordinate that incorporates the natural convection effect is used to well predict the intensity distribution of the probe beam after passing through liquid medium [13]. In this research, the pump power and propagation distance are controlled to investigate the probe beam profile influence on the thermal lens effect both experimentally and theoretically.

Flat-top laser are well known to present significant advantages for laser technology, such as holographic recording system, Z-scan measurement, laser heat treatment and surface annealing in microelectronics and various nonlinear optical processes [14–18]. For CW beams, several approaches to spatially shape Gaussian beams have been developed, such as the use of aspheric lenses, implement beam shaping or the use of diffractive optical devices [19]. However, these methods have some disadvantages: a refractive beam shaping system lead to large aberration [20]; the implemental beam shaping has low energy efficiency and lacks of flexibility [21]; and the use of refractive optical devices requires complex configuration design and high cost [22]. In practice, a low-cost and flexible method to convert a Gaussian beam into a flat-top beam is required. In this research, a novel fluidic laser beam shaper is demonstrated.

* Corresponding author.
E-mail address: doan.d.aa@m.titech.ac.jp (H.D. Doan).

0017-9310/$ - see front matter © 2012 Elsevier Ltd. All rights reserved.
doi:10.1016/j.ijheatmasstransfer.2012.02.029

Nomenclature

a	thermal diffusivity (m^2/s)
c	concentration (mol/L)
d	distance from the sample to the detector of the CCD camera (m)
g	acceleration of gravity (m/s^2)
k_0	free space wave number (m^{-1})
I_0	intensity of the laser (W/m^2)
L	sample thickness (m)
n	refractive index of liquid medium
n_0	refractive index of liquid medium at 20 °C
R	radius of curvature of the wave front
p	pressure (Pa)
P	power of laser (W)
S	heat source (K/s)
T	temperature (K)
r, r', z	coordinate (m)
v_r, v_z	velocity in r, z direction (m/s)
r_0	beam radius (m)

Greek symbols

α	absorption coefficient (cm^{-1})
β	coefficient of volume expansion, (K^{-1})
λ	laser beam wavelength (nm)
ρ	density of liquid medium, (kg/m^3)
Φ	beam waist (FWHM) (m)
θ	divergence of the laser beam (mrad)
ν	kinematic viscosity (m^2/s)

2. Principle of thermal lens effect

In this study, it is assumed that the change of refractive index is caused only by the temperature change of the liquid medium and the thermal coefficient of the refractive index, dn/dT. The concentrations are supposed to be constant over the range of the temperature rise induced by the pump beam. When the liquid medium is irradiated, temperature distribution perpendicular to the optical axis is formed due to intensity distribution of laser beam and heat transport. To consider the natural convection effect, the temperature distribution of liquid sample in steady state is calculated numerically in 2D cylindrical axisymmetrical coordinate following these governing equations [13]:

$$\frac{1}{r}\frac{\partial}{\partial r}(rv_r) + v_z\frac{\partial v_z}{\partial z} = 0 \tag{1}$$

$$v_r\frac{\partial v_r}{\partial r} + v_z\frac{\partial v_r}{\partial z} = -\frac{1}{\rho}\frac{\partial p}{\partial r} + \nu\left(\frac{\partial}{\partial r}\left(\frac{1}{r}\frac{\partial}{\partial r}(rv_r)\right) + \frac{\partial^2 v_r}{\partial z^2}\right) \tag{2a}$$

$$v_r\frac{\partial v_z}{\partial r} + v_z\frac{\partial v_z}{\partial z} = -\frac{1}{\rho}\frac{\partial p}{\partial z} + \nu\left(\frac{1}{r}\frac{\partial}{\partial r}\left(r\frac{\partial v_z}{\partial r}\right) + \frac{\partial^2 v_z}{\partial z^2}\right) + g\beta(T - T_0) \tag{2b}$$

$$v_r\frac{\partial T}{\partial r} + v_z\frac{\partial T}{\partial z} = a\left(\frac{1}{r}\frac{\partial}{\partial r}\left(r\frac{\partial T}{\partial r}\right) + \frac{\partial^2 T}{\partial z^2}\right) + S \tag{3}$$

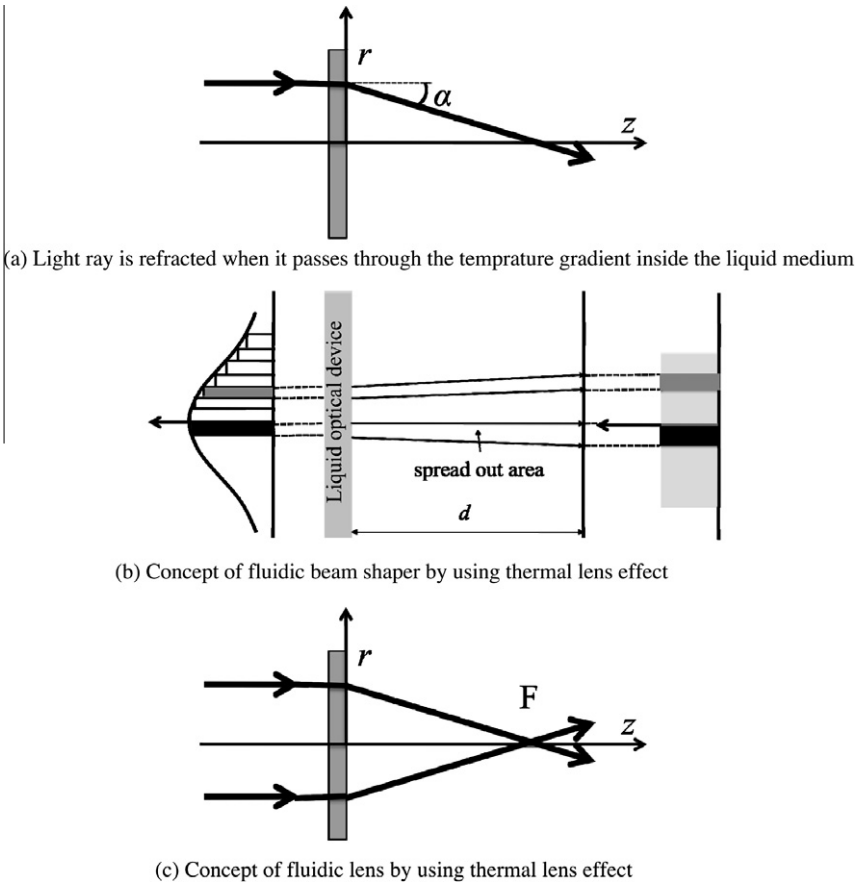

(a) Light ray is refracted when it passes through the temprature gradient inside the liquid medium

(b) Concept of fluidic beam shaper by using thermal lens effect

(c) Concept of fluidic lens by using thermal lens effect

Fig. 1. Image of fluidic optical devices.

$$S = \frac{\alpha e^{-\alpha z} I_0(r)}{\rho C_p} \quad (4)$$

Here, $I_0(r)$ is the intensity distribution of the pump laser. The spot sizes of the laser beams are assumed to be constant through the interaction volume within the liquid medium.

The temperature distribution is calculated numerically base on finite difference method. The 1st order upwind scheme and a 2nd order center differencing are applied to discretise the advection term and the diffusion term respectively. The thermal properties of liquid medium can be found in Table 1.

To model the propagation of laser through inhomogeneous medium, the wave equation including an absorption term and an inhomogeneous refractive index term is applied:

$$-\frac{\partial^2 E}{\partial z^2} + 2ik_0 n_0 \frac{\partial E}{\partial z} = \frac{1}{r}\frac{\partial}{\partial r}\left(\frac{\partial (rE)}{\partial r}\right) + k_0^2 (n^2 - n_0^2)E - \frac{1}{2} ik_0 n_0 \alpha E \quad (5)$$

Here, E is the envelope of the oscillating electric field, z is the axis of propagation, r is transverse coordinates, k_0 is the free space wave number and α is the absorption coefficient. The variable n is the refractive index profile depending on medium temperature following:

$$n(T) = n_0 + \frac{dn}{dT}(T - T_0) \quad (6)$$

Here, $n_0 = 1.359$ is the refractive index of the liquid medium at reference temperature $T_0 = 298.15$ K, dn/dT is the temperature coefficient of the refractive index. The propagation of laser is calculated base on Pade method. The optical properties parameter can be found in Table 1.

3. Influences of the pump power and the propagation distance on the change of probe beam profile

Influences of the pump power and the propagation distance to the probe beam profile were investigated numerically using the calculation parameters in Table 2. In this calculation, both of pump beam and probe beam are written as follows.

$$E = E_0 \exp\left(\frac{-r^2}{r_0^2}\right) \exp\left(\frac{-ik_0 n_0 r^2}{2R}\right) \quad (7)$$

$$E_0 = \sqrt{\frac{2P}{\pi r_0^2}} \quad (8)$$

Here P is the power of laser, R is the radius of curvature of the wave front, r and r_0 are distance from laser axis and beam radius respectively.

Effects of the pump power and the propagation distance to the probe beam profile are shown in Figs. 2(a) and (b) respectively. The vertical axis and horizontal axis show intensity and distance from laser axis respectively. Plots of '$P = 0$ mW' and '$d = 0$ mm' represent intensity distribution of the probe beam without thermal lens effect. As shown in Fig. 2(a), the further the propagation distance, the lower intensity at the probe beam center, and higher intensity at the wing. With increasing of the propagation distance, the laser beam profile changes from Gaussian to flat-top and the doughnut beam profile respectively. The profile of the probe beam changes with the same tendency as the increasing of pump power as shown in Fig. 2(b). In particular, when the pump power is 3 mW and propagation distance is 200 mm the probe beam is converted to the flat-top profile approximately. Therefore, by controlling the pump power and the propagation distance the Gaussian beam can be converted into the flat-top beam.

Table 1
Calculation conditions.

Parameter	Unit	Value
Thermal conductivity, k	[W/(m K)]	0.167
Kinematic viscosity, v	[m^2/s]	1.334×10^6
Coefficient of volume expansion, β	[K^{-1}]	1.04×10^{-3}
Density, ρ	[kg/m^3]	789
Specific heat, C_p	[J/(kg K)]	2460
Absorption coefficient, α	[cm^{-1}]	2.92
Refractive index change, dn/dT	[K^{-1}]	-3.97×10^{-4}

Table 2
Calculation conditions.

Parameter	(a)	(b)
Pump power, mW	3	0–7
Pump beam diameter, mm	0.8	0.8
Probe power, mW	10	10
Probe beam diameter, mm	0.8	0.8
Absorption coefficient, cm^{-1}	2.0	2.0
Distance from experimental section to CCD camera, mm	0–500	200
Phase front curvature radius, R, mm	∞	∞

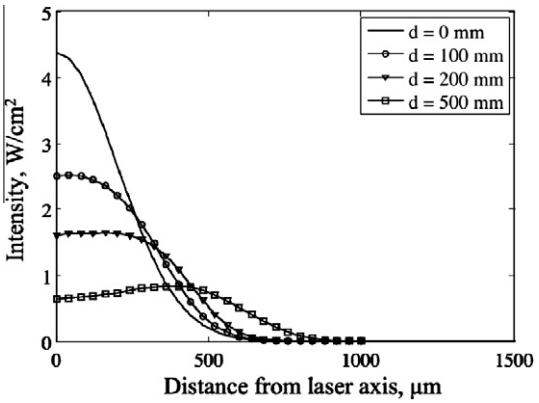

Fig. 2a. Influence of the propagation distance to the probe beam profile. The vertical and horizontal axes show intensity and distance from laser axis respectively. '$d = 0$ mm' represents the intensity distribution of the probe beam without thermal lens effect.

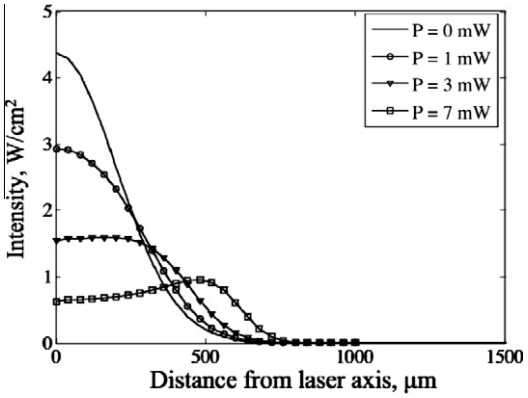

Fig. 2b. Influence of the pump power to the probe beam profile. The vertical and horizontal axes show intensity and distance from laser axis respectively. '$P = 0$ mW' represents intensity distribution of the probe beam without thermal lens effect.

4. Experimental set-up to shape spatial profile

In order to confirm the role of the fluidic laser beam shaper, a single-beam experiment is set up as shown in Fig. 3. A CW diode

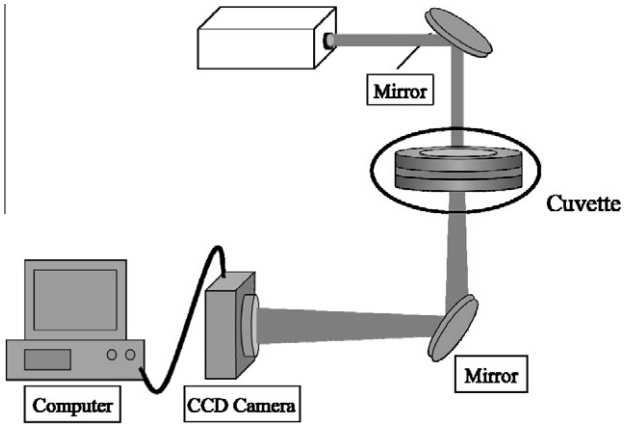

Fig. 3. Experimental set up for single beam system.

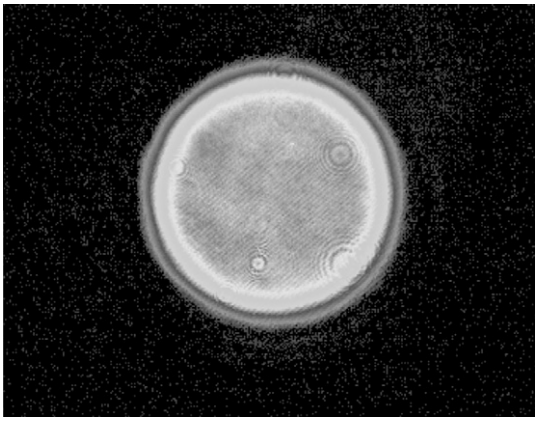

Fig. 5a. Flat-top beam profile measured by CCD camera at the propagation distance of 150 mm from the cuvette (absorption coefficient of 2.92 cm^{-1}).

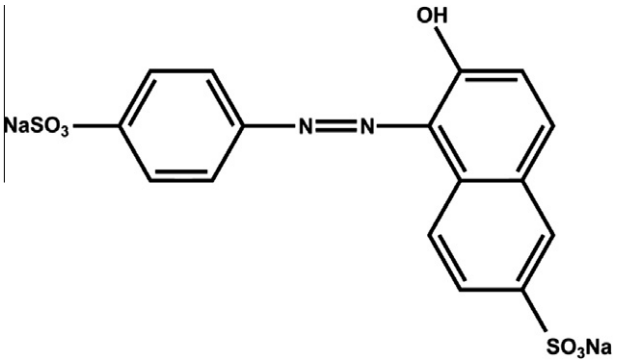

Fig. 4. Molecular formula of the Sunset-yellow.

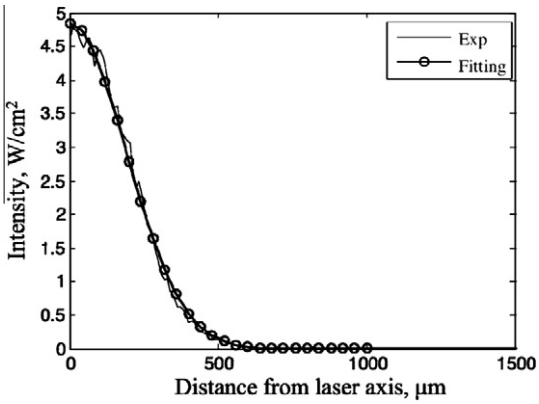

Fig. 5b. The fitting of laser beam profile measured at the surface of the cuvette by using Eq. (7), (8) with $P = 11$ mW, $r_0 = 0.38$ mm and $R = 320$ mm respectively.

blue laser is used as pump and probe-beam ($P = 10$ mW, $\lambda = 488$ nm, $\Phi = 0.69$ mm, TEM00). A CCD camera is used as a detector to measure the intensity distribution of the laser beam. A cuvette, a three-layer structure with a sheet copper is sandwiched between two pieces of fused silica. The thickness of the fused silica is 1 mm. The sheet copper has doughnut shape. The liquid that is contained inside the doughnut hole has the same hight with the sheet copper. By varying the thickness of the sheet copper, the liquid hight can be changed. The ethanol solution dissolved dye termed as Sunset-yellow is filled in the cuvette. The chemical formula of the Sunset-yellow is shown in Fig. 4. In this experiment, the hight of the liquid medium is 0.5 mm, the dye concentration is 0.1 g/l and the absorption coefficient is 2.92 cm^{-1} (measured value) respectively. The propagation distance to obtain the flat-top beam profile is measured by changing the distance from the cuvette to the CCD camera. At the propagation distance of 150 mm, the flat-top beam is confirmed as shown in Fig. 5(a).

Fig. 5(b) shows the fitting of laser beam profile measured at the surface of the cuvette by using Eq. (7), (8) with $P = 11$ mW, $r_0 = 0.38$ mm and $R = 320$ mm. Here, the radius of curvature of the beam's wave front at the cuvette surface, R, is calculated base on divergence of the laser beam $\theta = 0.95$ mrad. The fitting value is used for the input of electric field in calculation. Fig. 5(c) shows the beam profile change from the Gaussian to the flat-top beam. The vertical and horizontal axes show the intensity and distance from the laser axis respectively. The *o*-line shows the profile of the Gaussian input beam by fitting the laser beam profile measured at the surface of the cuvette. The strange-line shows the profile of the flat-top beam calculated by beam propagation method. The solid-line shows the profile of the flat-top beam measured by CCD camera at propagation distance of 150 mm from the cuvette. Both experimental and calculated results agree well with each other.

In order to explain more detail about the mechanism of this fluidic beam shaper, the temperature distribution of liquid medium is calculated. As shown in Fig. 6, local heating near the beam axis produces a radially dependent temperature variation, which changes the liquid refractive index in which the lower refractive index is in the region near to the beam center. As a consequence, the radius of curvature of the wave front at the region near the beam center is shorter than one at the beam wing. Therefore the sample liquid locally acts as a micro divergent lens with shorter focal length at beam center. As shown in Fig. 1b, the beam center which passing through shorter focal length is spread out more rapidly than the beam wing. As the probe beam propagates to increasing distance, the intensity in the center region drops rapidly than one in the wing region. At a certain value of propagation distance, the Gaussian beam can be converted into the flat-top beam.

It is noted that, in the case of single-beam shaper, one part of laser beam energy (about 15% in this experiment) is converted into thermal energy in order to change temperature distribution or in other words to change refractive index distribution in the liquid medium. Therefore, in the case of single-beam shaper, the beam shaper has another role, which is as an attenuator. This laser beam shaper/attenuator can be applied in practical laser drilling technology. In the case of applying on only laser beam shaper, the double-beam system is recommended. In this case, it is needed to select dye whose absorbance of the probe-beam is negligible small.

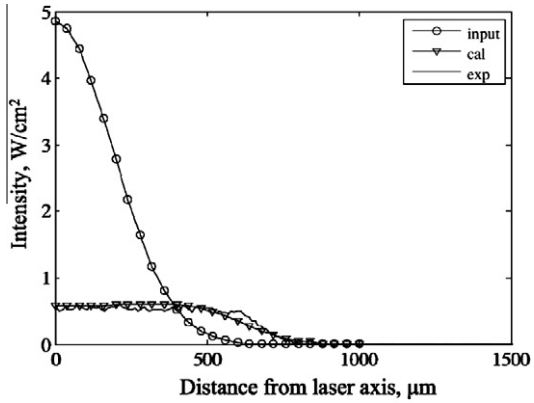

Fig. 5c. Beam profile change from the Gaussian to the flat-top beam. The vertical and horizontal axes show intensity and distance from the laser axis respectively. The *o*-line shows the profile of the Gaussian input beam by fitting the laser beam profile measured at the surface of the cuvette. The strange-line shows the profile of the flat-top beam calculated by beam propagation method. The solid-line shows the profile of the flat-top beam measured by CCD camera at propagation distance of 150 mm from the cuvette.

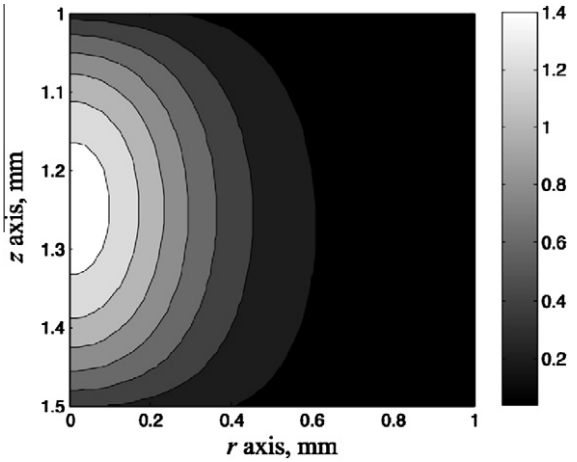

Fig. 6. Temperature distribution inside the liquid medium [K]. The calibration shows the difference between temperature inside the liquid medium with the ambient temperature.

5. Relationship between pump power and distance to shape spatial profile

As shown in previous section, the flat-top beam can be obtained only at a fixed distance. In order to control this distance, the influence of pump power is investigated theoretically and experimentally. The calculation parameters are shown in Table 3. Pump power is changed from 1 to 8 mW. The distance to obtain the flat-top beam is obtained numerically. The relationship between the pump power and the distance to shape spatial profile is shown in Fig. 7. The horizontal and vertical axes show pump power and distance to obtain the flat-top beam respectively. As shown in Fig. 7, the distance to obtain a flat-top beam is in inverse proportion to pump power. To validate the numerical prediction, a single beam experiment was carried out. The pump power is changed from 1 to 6 mW and the distance to obtain the flat-top beam was measured. The experimental result shown in Fig. 8, shows the excellent agreement with calculation prediction. The relationship between pump power and distance to obtain the flat-top beam can be explained by the interaction between energy absorption

Table 3
Calculation conditions.

Parameter	(b)
Pump power, mW	1–8
Pump beam diameter, mm	0.8
Probe power, mW	10
Probe beam diameter, mm	0.8
Absorption coefficient, cm^{-1}	2.0
Phase front curvature radius, *R*, mm	320

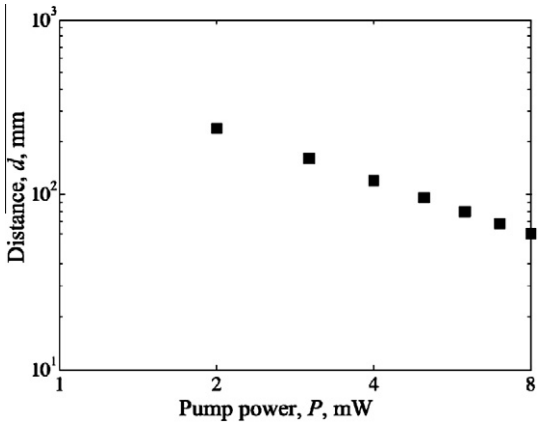

Fig. 7. Relationship between the pump power and the distance to obtain the flat-top beam predicted by calculation. The horizontal and vertical axes show the pump power and distance to obtain the flat-top beam respectively. Pump power is changed from 1 to 8 mW.

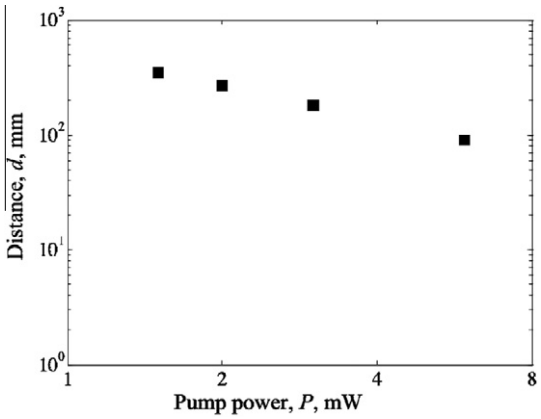

Fig. 8. Relationship between the pump power and the distance to obtain the flat-top beam profile measured by single beam experiment. The horizontal and vertical axes show pump power and distance to obtain the flat-top beam profile respectively. Pump power is changed from 1 to 6 mW.

of liquid medium with the focal length of local micro lens. As the pump power increase, the absorption energy increases. As a consequence, the rate of decreasing of *R* is enhanced. This can be thought as the reason why the distance to obtain a flat-top beam decreases. In other words, the distance to obtain the flat-top beam profile also decreases with the increasing of absorption coefficient. Therefore, by changing the absorption coefficient or the pump power, the distance to obtain a flat-top beam can be controlled.

6. Conclusions

In this research, a novel idea of fluidic beam shaper is demonstrated. The fluidic beam shaper is based on controlling some

parameters in the thermal lens system. The interaction among the pump power, the absorption coefficient and the distance to obtain the flat-top beam profile have been investigated experimentally and theoretically. It is found that, by controlling the pump power (in the regime of linear optics) and the absorption coefficient, the input Gaussian beam can be converted into a flat-top beam profile. The distance to get the flat-top beam profile can be controlled easily by adjusting the pump power and the absorption coefficient. In actually application, single-beam shaper has another role, which is as an attenuator. This laser beam shaper/attenuator can be applied in practical laser drilling technology. In the case of applying on only laser beam shaper, the double-beam system is recommended. In this case, it is needed to select a dye whose absorbance of the probe-beam is negligible small. With some merits such as flexibility, versatility and low cost, this method will be a promising tool in many fields of laser application.

Acknowledgement

Part of this work has been supported by the Grant-in-Aid for JSPS Fellows and Grant-in-Aid for Scientific Research of MEXT/JSPS.

References

[1] J.P. Gordon, R.C.C. Leite, R.S. Moore, S.P.S. Porto, J.R. Whinnery, Long-transient effects in lasers with inserted liquid samples, J. Appl. Phys. 36 (1965) 3–8.
[2] S.A. Akhmanov, D.P. Krindach, A.V. Migulin, A.P. Sukhorukov, R.V. Khokhlov, Thermal self-actions of laser beams, IEEE J. Quant. Electron. QE-4 (1968) 568–575.
[3] P.M. Livingston, Thermally induced modifications of a high power CW laser beam, Appl. Opt. 10 (1971) 426–436.
[4] J.F. Power, Pulsed mode thermal lens effect detection in the near field via thermally induced probe beam spatial phase modulation: a theory, Appl. Opt. 29 (1990) 52–63.
[5] P.P. Banerjee, R.M. Misra, M. Maghraoui, Theoretical and experimental studies of propagation of beams through a finite sample of a cubically nonlinear material, J. Opt. Soc. Am. B 8 (1991) 1072–1080.
[6] J.M. Hickmann, A.S.L. Gomes, C.B. de Araújo, Observation of spatial cross-phase modulation effects in a self-defocusing nonlinear medium, Phys. Rev. Lett. 68 (1992) 3547–3550.
[7] Govind P. Agrawal, Transverse modulation instability of copropagating optical beams in nonlinear Kerr media, J. Opt. Soc. Am. B 7 (1990) 1072–1078.
[8] C.J. Rosenberg et al., Analysis of the dynamics of high intensity Gaussian laser beams in nonlinear de-focusing Kerr media, Optics Comm. 275 (2007) 458–463.
[9] M. Sakakura, M. Terazima, Oscillation of the refractive index at the focal region of a femtosecond laser pulse inside a glass, Opt. Lett. 29 (13) (2004) 1548–1550.
[10] M. Sakakura, M. Terazima, Real-time observation of photothermal effect after photo-irradiation of femtosecond laser pulse inside a glass, J. Phys. France 125 (2005) 355–360.
[11] M. Terazima, N. Hirota, S.E. Braslavsky, A. Mandelis, S.E. Bialkowski, G.J. Diebold, R.J.D. Miller, D. Fournier, R.A. Palmer, A. Tam, Quantities, terminology, and symbols in photothermal and related spectroscopies (IUPAC Recommendations 2004), Pure Appl. Chem. 76 p. 1083.
[12] H.D. Doan, K. Fushinobu, K. Okazaki, Investigation on the interaction among light, material and temperature field in the transient lens effect, transmission characteristics in 1D temperature field, Proc. ITherm. (127) (2010).
[13] D.H. Doan, M. Chijiiwa, K. Fushinobu, K. Okazaki, Investigation on the interaction among light, material and temperature field in the transient lens effect, propagation characteristics in 2D temperature field, Therm. Sci. Eng. 19 (2) (2011) 43–50.
[14] J. Yang, Y. Wang, X. Zhang, C. Li, X. Jin, M. Shui, Y. Song, Characterization of the transient thermal-lens effect using flat-top beam Z-scan, J. Phys. B At. Mol. Opt. Phys. 42 (2009) 225404. 5pp.
[15] K. Ebata, K. Fuse, T. Hirai, K. Kurisu, Advanced laser optics for laser material processing, Proc. SPIE 5063 (2003) 411.
[16] E.B.S. Govil, J.P. Longtin, A. Gouldstone, M.D. Frame, Uniform-intensity, visible light source for in situ imaging, J. Biomed. Optics 14 (2) (2009) 024024–024024-7.
[17] F.M Dickey, S.C Holswade, D.L Shealy, Laser Beam Shaping Applications', Taylor Francis, 2006.
[18] M.T. Eismann, A.M. Tai, J.N. Cederquist, Iterative design of a holographic beam former, Appl. Opt. 28 (1998) 1650–2641.
[19] F.M Dickey, S.C Holswade, Laser Beam Shaping: Theory and Techniques, Marcel Dekker, New York, 2000.
[20] P. Scott, Reflective optics for irradiance redistribution of laser beam design, Appl. Opt. 20 (9) (1981) 1606–1610.
[21] S. Zhang, Q. Zhang, G. Lupke, Spatial beam shaping of ultrashort laser pulse: theory and experiment, Appl. Opt. 44 (2005) 5818–5823.
[22] B. Mercier, J.P. Rousseau, A. Jullien, L. Antonucci, Nonlinear beam shaper for femtosecond laser pulses from Gaussian to flat-top profile, Optics Comm. 283 (2010) 2900–2907.